Genomic organization, gene expression and activity profile of *Marinobacter hydrocarbonoclasticus* denitrification enzymes

Cíntia Carreira [1,2] , **Olga Mestre** [1] , **Rute F. Nunes** [1] , **Isabel Moura** [2] , **Sofia R. Pauleta** [Corresp. 1]

[1] Microbial Stress Lab, UCIBIO, REQUIMTE, Departamento de Química, Faculdade de Ciências e Tecnologia, Universidade Nova de Lisboa, Caparica, Portugal

[2] Biological Chemistry Lab, LAQV, REQUIMTE, Departamento de Química, Faculdade de Ciências e Tecnologia, Universidade Nova de Lisboa, Caparica, Portugal

Corresponding Author: Sofia R. Pauleta
Email address: srp@fct.unl.pt

Background. Denitrificationis one of the main pathways of the N-cycle, during which nitrate is converted to dinitrogen gas, in four consecutive reactions that are each catalyzed by a different metalloenzyme. One of the intermediate metabolites is nitrous oxide, which has a global warming impact greater then carbon dioxide and which atmospheric concentration has been increasing in the last years. The four denitrification enzymes have been isolated and biochemically characterized from *Marinobacter hydrocarbonoclasticus* in our lab.

Methods. Bioinformatic analysis of the *M. hydrocarbonoclasticus* genome to identify the genes involved in the denitrification pathway. The relative gene expression of the gene encoding the catalytic subunits of those enzymes was analyzed during the growth under microoxic conditions. The consumption of nitrate and nitrite, and the reduction of nitric oxide and nitrous oxide by whole-cells was monitored during anoxic and microoxic growth in the presence of 10 mM sodium nitrate at pH 7.5.

Results . The bioinformatic analysis shows that genes encoding the enzymes and accessory factors required for each step of the denitrification pathway are clustered together. An unusual feature is the co-existence of genes encoding a *q*- and a *c*-type nitric oxide reductase, with only the latter being transcribed at similar levels as the ones encoding the catalytic subunits of the other denitrifying enzymes, when cells are grown in the presence of nitrate under microoxic conditions. Using either a batch- or a closed system, nitrate is completely consumed in the beginning of the growth, with transient formation of nitrite, and whole-cells can reduce nitric oxide and nitrous oxide from mid-exponential phase until being collected (time-point 50 h).

Discussion . *M. hydrocarbonoclasticus* cells can reduce nitric and nitrous oxide *in vivo,* indicating that the four denitrification steps are active. Gene expression profile together with promoter regions analysis indicates the involvement of a cascade regulatory mechanism triggered by FNR-type in response to low oxygen tension, with nitric oxide and nitrate as secondary effectors, through DNR and NarXL, respectively. This global characterization of the denitrification pathway of a strict marine bacterium, contributes to the understanding of the N-cycle and nitrous oxide release in marine environments.

1   **Genomic organization, gene expression and activity profile of *Marinobacter***

2   ***hydrocarbonoclasticus* denitrification enzymes**

4   Cíntia Carreira[1,2], Olga Mestre[1], Rute F. Nunes[1], Isabel Moura[2], Sofia R. Pauleta*[1]

6   [1] Microbial Stress Lab, UCIBIO, REQUIMTE, Departamento de Química, Faculdade de

7   Ciências e Tecnologia, Universidade Nova de Lisboa, Campus da Caparica, 2829-516 Caparica,

8   Portugal.

9   [2] Biological Chemistry Lab, LAQV, REQUIMTE, Departamento de Química, Faculdade de

10   Ciências e Tecnologia, Universidade Nova de Lisboa, Campus da Caparica, 2829-516 Caparica,

11   Portugal.

17   **Corresponding Author**

18   Sofia R. Pauleta

19   Microbial Stress Lab, UCIBIO, REQUIMTE, Departamento de Química, Faculdade de Ciências

20   e Tecnologia, Universidade Nova de Lisboa, Campus da Caparica, 2829-516 Caparica, Portugal.

21   Email: srp@fct.unl.pt

22   Tel. +351 212 948 385, ext. 10967

23   Fax: + 351 212 948 550

25   **Abstract**

26   **Background.** Denitrification is one of the main pathways of the N-cycle, during which nitrate is

27   converted to dinitrogen gas, in four consecutive reactions that are each catalyzed by a different

28   metalloenzyme. One of the intermediate metabolites is nitrous oxide, which has a global

29   warming impact greater then carbon dioxide and which atmospheric concentration has been

30   increasing in the last years. The four denitrification enzymes have been isolated and

31   biochemically characterized from *Marinobacter hydrocarbonoclasticus* in our lab.

32   **Methods.** Bioinformatic analysis of the *M. hydrocarbonoclasticus* genome to identify the genes

33   involved in the denitrification pathway. The relative gene expression of the gene encoding the

34   catalytic subunits of those enzymes was analyzed during the growth under microoxic conditions.

35   The consumption of nitrate and nitrite, and the reduction of nitric oxide and nitrous oxide by

36   whole-cells was monitored during anoxic and microoxic growth in the presence of 10 mM

37   sodium nitrate at pH 7.5.

38   **Results**. The bioinformatic analysis shows that genes encoding the enzymes and accessory

39   factors required for each step of the denitrification pathway are clustered together. An unusual

40   feature is the co-existence of genes encoding a *q*- and a *c*-type nitric oxide reductase, with only

41   the latter being transcribed at similar levels as the ones encoding the catalytic subunits of the

42   other denitrifying enzymes, when cells are grown in the presence of nitrate under microoxic

43   conditions. Using either a batch- or a closed system, nitrate is completely consumed in the

44   beginning of the growth, with transient formation of nitrite, and whole-cells can reduce nitric

45   oxide and nitrous oxide from mid-exponential phase until being collected (time-point 50 h).

46   **Discussion**. *M. hydrocarbonoclasticus* cells can reduce nitric and nitrous oxide *in vivo*,

47   indicating that the four denitrification steps are active. Gene expression profile together with

48 promoter regions analysis indicates the involvement of a cascade regulatory mechanism

49 triggered by FNR-type in response to low oxygen tension, with nitric oxide and nitrate as

50 secondary effectors, through DNR and NarXL, respectively. This global characterization of the

51 denitrification pathway of a strict marine bacterium, contributes to the understanding of the N-

52 cycle and nitrous oxide release in marine environments.

53

54

55

Introduction

Under anoxic conditions, some organisms can use nitrate or nitrite as the sole electron acceptor in a pathway known as denitrification. This pathway allows the generation of an electrochemical gradient across the inner membrane, leading to energy conservation and ATP synthesis (Zumft 1997).

The denitrification pathway is composed of four consecutive reactions, each catalyzed by a different metalloenzyme, that in different organisms can be catalyzed by more than one metalloenzyme (Table S1 in Supplementary Information), and only the co-existence of *nar* and *nap*, encoding nitrate reductases, has been reported in some bacteria (Heylen et al. 2007). These steps are the reduction of nitrate to nitrite, by nitrate reductase (NaR), then to nitric oxide (NO), by nitrite reductase (NiR), to nitrous oxide (N_2O) by nitric oxide reductase (NOR) and, finally, to molecular dinitrogen, a reaction catalyzed by nitrous oxide reductase (N_2OR) (Zumft 1997).

The genes encoding these enzymes and some of the accessory factors, involved in the biosynthesis of their active centers are located in close proximity and are sometimes transcribed as polycistronic units (Pauleta et al. 2013; Zumft 1997). The regulatory network of those genes is complex and vary between organisms, but signals as oxygen, nitrate/nitrite, NO and cell redox changes are usually implied in triggering a cascade of transcription factors able to activate or repress the promoters of denitrification genes. Although the regulatory mechanisms are not completely understood, some proteins, such as fumarate-nitrate reduction regulator (FNR), dissimilatory nitrate respiration regulator (DNR) and nitrite and nitric oxide regulator (NNR) or their orthologs, that sense those signals through iron-sulfur centers or hemes, bind DNA sequences at the promoters regions of the denitrification genes (Spiro 2012).

Moreover, most of the studies on the denitrification pathway have been focused on Gram-

79   negative bacteria that occupy terrestrial niches, using *Paracoccus denitrificans* (alpha-

80   proteobacteria), *Pseudomonas stutzeri* and *Pseudomonas aeruginosa* (gamma-proteobacteria), as

81   model organisms (2017; Eady et al. 2016; Stein & Klotz 2011). There are still few studies on the

82   identification and diversity of genes involved in denitrification in other families of bacteria,

83   especially marine bacteria, which could in part be related to a restricted number of denitrifying

84   isolates and of complete genomes. Nevertheless, this group of microorganisms is having an

85   increased attention in the latest years with some studies being reported recently (Laass et al.

86   2014; Mauffrey et al. 2017; Mauffrey et al. 2015).

87   The release of nitrous oxide to the atmosphere is in large extent due to anthropogenic activities,

88   such as industrial and agriculture, but the natural sources (soil and ocean) also play a role, which

89   has led to an increasing number of studies on the nitrogen cycle, and especially on the

90   denitrification pathway. However, many of these studies were performed on bacteria that occupy

91   terrestrial niches, leaving marine bacteria without the proper attention. Therefore, and since a

92   large amount of nitrous oxide released from natural sources comes from the ocean (Bange 2006),

93   there is a need to characterize the denitrification pathway of marine bacteria.

94   *Marinobacter* spp. are ubiquitous in marine environments, being found in different depths in the

95   oceans and marine ecosystems (Kaye & Baross 2000; Yoon et al. 2003) and so far, three strains

96   of *M. hydrocarbonoclasticus* had its genome sequenced (Grimaud et al. 2012; Ling et al. 2017;

97   Singer et al. 2011) (note that *Marinobacter aquaeolei* is a *M. hydrocarbonoclasticus* strain

98   (Marquez & Ventosa 2005)). This microorganism is proposed to have a high impact on the

99   different biogeochemical cycles (Singer et al. 2011), including the N-cycle, and have a versatile

100   metabolism in terms of carbon source and can use either nitrate/nitrite and/or oxygen as electron

101   acceptors. *M. hydrocarbonoclasticus* is a moderate halophilic, and thus can be potentially used in

102 wastewater plans with high saline content, for which its role as a denitrifier is crucial to remove

103 nitrate and nitrite content from industrial sources (Li et al. 2013). *M. hydrocarbonoclasticus* 617

104 was chosen for the work presented here, given that all of the metalloenzymes from this pathway

105 have already been characterized in our laboratory (Correia et al. 2008; Lopes et al. 2001;

106 Prudêncio et al. 2000; Timoteo et al. 2011). The nitrate reductase is encoded by the *nar* operon,

107 being a membrane enzyme with a molybdenum center, that receives electrons from the quinol

108 pool (Correia et al. 2008). Reduction of nitrite in this organism is catalyzed by nitrite reductase

109 cytochrome cd_1 (Lopes et al. 2001), releasing nitric oxide that is reduced by the membrane nitric

110 oxide reductase *c*-NOR, which has two subunits, one containing a *c*-type heme, named NorC and

111 NorB where the catalytic center is located (Timoteo et al. 2011). The last step of the

112 denitrification is catalyzed by nitrous oxide reductase, which is a copper enzyme containing a

113 CuA and a CuZ center (Dell'acqua et al. 2008; Dell'Acqua et al. 2012). These last three enzymes

114 receive electrons from the periplasmic cytochrome c_{552}, forming transient electron transfer

115 complexes (Dell'acqua et al. 2011; Ramos et al. 2017) (Figure 1).

116 Here, the genome of *M. hydrocarbonoclasticus* SP17 was analyzed in detail to identify the

117 location of genes encoding the catalytic domains of the denitrifying enzymes and of the

118 accessory factors proposed to be involved in their biosynthesis or in maintaining the enzymes in

119 an active state. Expression profiling of genes encoding these enzymes was performed during *M.*

120 *hydrocarbonoclasticus* 617 growth in microoxic denitrifying conditions. The activity profile of

121 the denitrifying enzymes and metabolites (nitrate/nitrite) was analyzed for cells cultured in a

122 batch system under microoxic conditions and in sealed serum flasks. In addition, the affinity of

123 the whole-cells for N_2O was examined.

124

125

126

Materials and Methods

128

Genome analysis

The genome sequence of *M. hydrocarbonoclasticus* SP17 (Grimaud et al. 2012), with the accession number NC_017067 (NCBI) was analyzed using bioinformatic tools to search for homologous genes encoding the catalytic subunits of the four enzymes that catalyze each step of the denitrification pathway, as well as accessory factors (see Supplementary Information S2). The virtual Footprint of PRODORIC database was used to detect the putative binding sites for FNR and IHF in the promoter regions of the denitrification genes (Table S3 in Supplementary Information). As a remark, the genomic organization of denitrification genes was analyzed using the deposited genome of *M. hydrocarbonoclasticus* SP17, while the strain that was cultured was *M. hydrocarbonoclasticus* 617. In fact, *nos* gene cluster had been sequenced in our lab (GenBank: DQ504302.1) and showed to have an identical organization including *dnr* gene upstream *nos* gene cluster.

141

***Marinobacter hydrocarbonoclasticus* 617 growth conditions**

M. hydrocarbonoclasticus 617 was grown in artificial seawater (ASW) liquid medium containing 1.17 % (w/v) NaCl, 0.075 % (w/v) KCl, 0.3 % (w/v) NH$_4$Cl, 1.23 % (w/v) MgSO$_4$.7H$_2$O, 0.6 % (w/v) Tris, 0.1 % (w/v) yeast extract and 0.12 % (w/w) sodium lactate as energy and carbon source (Baumann & Baumann 1986). The pH was adjusted to 7.5 with 37 % (w/w) HCl. The medium was supplemented with 0.33 mM K$_2$HPO$_4$, 10 mM CaCl$_2$.2H$_2$O, 7.2 μM FeSO$_4$.7H$_2$O

148 and a Starkey oligoelement solution (Starkey 1938) (1 mL/L of culture), with the composition

149 listed in Supplementary Information S4.

150

151 *(i) Growth in 2-L bioreactors*

152 In the pre-inocula required prior to the inoculation of the 2-L bioreactor, bacteria were grown

153 under oxic conditions for 24 h at 30 ºC, 210 rpm. The first pre-inoculum was prepared by

154 inoculating 5 mL ASW liquid medium with bacteria maintained in ASW agar plates. This culture

155 was then used to inoculate 50 mL ASW liquid medium and finally 500 mL ASW liquid medium.

156 200 mL of this final culture was used to inoculate 1.8 L of medium in a 2-L bioreactor. *M.*

157 *hydrocarbonoclasticus* was grown in the bioreactor in a batch mode for approximately 48 h at 30

158 °C, using 0.75 % (w/w) sodium lactate as carbon source and 10 mM sodium nitrate, as electron

159 acceptor. The pH was continuously monitored and maintained at 7.5. A low aeration rate (0.2

160 vvm) and an agitation speed of 150 rpm were used during 5 h, and then it was decreased to 50

161 rpm. The oxygen concentration in the culture medium was monitored with a InPro 6950i G Trace

162 Oxygen Sensor (Mettler Toledo). The growth started with an oxygen saturated medium (100 %)

163 and after approximately 2 h the oxygen levels reached 0 % (see Supplementary Information

164 Figure S1). Cultures were visualized under an optical microscope to detect any contamination

165 with microorganisms with a different morphology. Bioreactor growth was performed at least in

166 triplicate. Bacterial growth in the bioreactor was monitored by collecting 4 mL aliquots into

167 sterile vials (see Supplementary Information S5), from which optical density at 600 nm

168 (OD_{600nm}) was measured. These aliquots were also used to quantify expression of the genes

169 encoding the catalytic subunits of the denitrification enzymes, as well as to determine nitrite and

170 nitrate levels and for the activity assays (see below). The aliquots were stored in liquid nitrogen

171   until further use, after dividing the samples for each application into different sterile vials.

172   *(ii) Growth in sealed serum flasks*

173   Denitrification pathway was also analyzed in the absence of aeration at pH 7.5 using 100 mL

174   sealed serum flasks (growth media was flushed with Argon prior to autoclave and sealed with a

175   rubber septum and aluminium caps) containing 50 mL AWS liquid medium, supplemented as

176   described above. The oxically grown inoculum was transferred (10 % of total volume) with a

177   syringe to the gas-tight vials. Similar conditions to the bioreactor growth were used with the

178   following modifications: there was no aeration during the growth, the pH was continuously

179   monitored but not adjusted (pH changed from 7.30 to 7.65) and cultures were stirred in a shaker

180   (at 150 rpm for 5 h and then changed to 50 rpm for the remaining duration of the growth), at 30

181   ºC. At each time-point, aliquots of 0.75 mL were sampled to measure the cell densities at 600

182   nm, quantify nitrate and nitrite and determine the rates of nitric oxide and nitrous oxide reduction

183   by the cells (see below). Sampling was performed under sterile conditions.

184

185   **Nucleic acid extraction and cDNA generation**

186   Samples of bioreactor cultures taken at different time-points were immediately frozen in liquid

187   nitrogen, until further use (1 mL). Total RNA, from the samples, was isolated using the Isolate II

188   RNA mini kit (Bioline), according to manufacturer's instructions. Genomic DNA contamination

189   was removed by on-column digestion with DNase I, supplied with the kit. RNA yields were

190   determined at 260 nm and purity was estimated by determining the A_{260nm}/A_{280nm} and

191   A_{260nm}/A_{230nm} ratios. To generate cDNA, 500 ng of each RNA sample (after its extraction) was

192   reversely transcribed using the SensiFAST cDNA Synthesis Kit (Bioline), using the following

193   conditions: 10 min at 25 °C, followed by 15 min at 42 °C and 5 min at 85 °C (for enzyme

194   inactivation). cDNAs were diluted (1:100) and stored at -80 °C until further use. DNA used in

195   standard curves was extracted from a sample of the bioreactor culture taken during the

196   exponential phase, using the Isolate II Genomic DNA Kit (Bioline), according to the

197   manufacturer's instructions and stored and -80 ºC until further use.

198

199   **Quantitative Real-Time PCR**

200   The expression of *M. hydrocarbonoclasticus* genes involved in the denitrification pathway -

201   *narG*, *nirS*, *c-norB* (*MARHYR3054*), *q-norB* (*MARHY3014*) and *nosZ* - was analyzed by

202   quantitative real-time PCR (qPCR). Reactions were performed using SensiFAST™ SYBR No-

203   ROX Kit (Bioline) with primers specific for each gene at 250 nM and 3 μL of cDNA. Gene

204   expression levels were determined using the relative standard curve method, which uses standard

205   curves to interpolate unknown quantity values from a sample. This was performed using DNA

206   standard curves, as previously described (Gomes et al. 2005). Briefly, for each target, as well as

207   for the control (16S rRNA), a standard curve was generated using serial dilutions of genomic

208   DNA. The amount of cDNA of each target and control gene, present in every sample, was

209   determined from their respective DNA standard curve, through conversion of the obtained

210   threshold cycle (C_t) value (Applied-Biosystems 2004; Gomes et al. 2005). Relative normalized

211   expression values were obtained by dividing the values obtained for each target gene by the

212   values obtained for the control gene (*16S rRNA*), as its expression is stable, during the different

213   growth phases. Primers were designed using Primer3 software (Untergasser et al. 2012) (Table

214   1). "No template" and "RT minus" (a Reverse Transcription reaction containing all reagents

215   except the reverse transcriptase enzyme) controls were also included in every PCR assay.

216   Reactions were run in a Corbett Rotor-Gene instrument (Qiagen) using the following thermal

217   cycling conditions: 95 °C for 5 min followed by 40 cycles of 95 °C for 15 s and 60 °C for 30 s.

218   Analysis of melting curves generated by the stepwise increase of the temperature from 60 °C to

219   95 °C, were used to verify the specificity of the amplified products. Three biological replicates

220   were analyzed but not at the exact same time points, thus a single representative experiment is

221   shown (similar results were obtained for the other replicates). Two to three technical replicates

222   were performed depending on the biological replicates.

223

224   **Co-transcriptional analysis of *nosRZDFYL***

225   To determine if *nosRZDFYL* is composed of a single transcriptional unit, a sample collected

226   during the exponential phase of *M. hydrocarbonoclasticus* growing in a bioreactor performed at

227   pH 7.5 was used. The cDNA was generated similarly to those described above but using 2 µg of

228   total RNA. PCR reactions were performed using 6 µL of the resulting cDNA and NZYTaq DNA

229   polymerase (Nzytech) with primer pairs that would amplify regions between *nosR* and *nosZ*

230   (nosR_F/nosZ_R), *nosZ* and *nosD* (nosZ_F/nosD_R) and *nosD* to *nosL* (nosD_F/nosL_R) (Table

231   1). Genomic DNA and a "RT minus" reactions were included as controls. The amplified PCR

232   products were analyzed by 1 % agarose gel electrophoresis, run at 100 V, during 20 min, and

233   visualized after incubation in a SYBR Safe solution (Invitrogen) under UV light.

234

235   **Nitrate/nitrite quantifications and nitric oxide and nitrous oxide reduction assays**

236   Nitrate and nitrite quantifications along the growth curve were performed using the

237   Nitrate/Nitrite Assay kit (Sigma), according to the manufacturer's instructions, in triplicate for

238   each time-point. The absorbance was measured at 540 nm in a VersaMax ELISA Microplate

239   Reader using the SoftMax Pro 6.4 software.

240 Whole-cell activity assays for nitric oxide and nitrous oxide reduction were performed

241 spectrophotometrically using a TIDAS diode array spectrophotometer, at RT inside an anaerobic

242 chamber (MBraun), by following the oxidation of reduced methyl viologen (non-physiologic

243 electron donor) at 600 nm, as previously described (Kristjansson & Hollocher 1980) (data

244 analysis is described in Supplementary Information S6). Nitric oxide (5% NO/95% He, Air

245 liquid) and nitrous oxide (> 95% N_2O, Air Liquid) solutions were freshly prepared before the

246 assays. Briefly, 5 mL of Milli-Q water were degassed for 30 min with Argon in sealed serum

247 flasks (sealed with a rubber septum and aluminium caps) and then flushed with N_2O for 1 h.

248 Taking into account the solubility of N_2O in water, at 25 °C and 1 atm, this solution is 25 mM in

249 N_2O (Kristjansson & Hollocher 1980). The NO solution was prepared similarly but a 10 % (per

250 mass) KOH solution was used between the NO bottle and the Milli-Q solution to remove other

251 nitrogen oxides from NO gas. A concentration of 1.91 mM in NO is reported at 20 °C for a 98.5

252 % NO stock, thus this solution is 9.7 µM (Timoteo et al. 2011). The assays were performed with

253 constant stirring by adding 40 µL cell suspension to a quartz cuvette already containing 120 µM

254 methyl viologen and 60 µM sodium dithionite in 100 mM Tris-HCl, pH 7.6 (in a final volume of

255 1 mL). The nitric oxide reduction assay was initiated by the addition of NO-saturated water to a

256 final concentration of 9.6 µM, while the nitrous oxide reduction assay was initiated (without any

257 further incubation) by the addition of N_2O-saturated water to obtain a 1.25 mM concentration in

258 the assay. The reduction rate (micromoles of NO or N_2O reduced per minute per optical density)

259 was obtained by analyzing the slope of the reaction after nitric oxide or nitrous oxide addition.

260 Controls of the reactions were performed in which nitric oxide or nitrous oxide were added to the

261 assay in the absence of cell suspension. In these controls no oxidation of MV was observed.

262 The dependence of N_2O in the reduction rate by whole-cells was performed in a 1 mL quartz

263 cuvette, containing 100 µM methyl viologen and 50 µM sodium dithionite in 100 mM Tris-HCl

264 pH 7.6, to which 3 µL of cells was added (containing 0.09 mg of total protein), collected by

265 centrifugation at the end of the growth performed at pH 7.5 in the bioreactor, under microoxic

266 conditions. The assay was initiated by the addition of 20, 40, 80, 120, 250 and 752 µM of N_2O-

267 saturated water. Triplicates for each substrate concentration were performed. Activities were

268 calculated as described above but reported as μmol_{N2O} min^{-1} mg^{-1} of total protein (determined

269 using the Pierce™ 660nm protein assay with bovine serum albumin as standard). The parameters

270 K_m and V_{max} were calculated by fitting the curve with the Michaelis-Menten equation.

271

272 **Results**

273 **Genomic organization of denitrification genes in *M. hydrocarbonoclasticus***

274 The genome of *M. hydrocarbonoclasticus* SP17 has several genes encoding proteins involved in

275 the different steps of the denitrification pathway clustered together (see Figure S3 in

276 Supplementary Information). The *nosZ*, encoding the catalytic unit of N_2OR, is included in the

277 *nosRZDFYL* gene cluster. Upstream the *nos* cluster is the NaR gene cluster, *narLXKGHJV* (see

278 Figure S3 in Supplementary Information), with *narG* encoding the catalytic subunit of NaR, and

279 *narXL*, the two-component system, NarXL, involved in transcriptional regulation of these genes

280 in response to nitrate and/or nitrite (Philippot 2002; Spiro 2012).

281 Several nitrate/nitrite transporters have been identified in the genome of *M.*

282 *hydrocarbonoclasticus*, one being associated with the *nar* cluster, other two upstream the *nir*

283 operon, and a *narU*-type gene is also annotated in this genome. Multiple NarK-like transporters

284 has also been identified in *P. aeruginosa* and *P. denitrificans* (Jia et al. 2009; Moir & Wood

285 2001), but their biological function is still a matter of debate, with different transports being

286   proposed to be required under specific growth conditions. The identification of the mechanism of

287   action of these membrane proteins can only be accomplished through the study of the physiology

288   of selected knock-out strains and site-directed mutagenesis.

289   Further upstream in the genome is *norBC*, encoding the two subunits of the short-chain

290   membrane-bound *c*-NOR (see Figure S3 in Supplementary Information). Neither *norE* nor *norF*

291   homologues were annotated in the genome of *M. hydrocarbonoclasticus*. However, the translated

292   sequence of *MARHY3057* shares 46 % sequence identity with *P. stutzeri* NorE (designated in

293   that microorganism as NirQ). A BLAST search was performed using the translated sequence of

294   *MARHY3058*, showing 53 % identity with *P. stutzeri* NirP (the NorF homologue in

295   *Pseudomonas* species with 82 residues), though in a very restricted region, covering only 49 %

296   of the primary sequence. Indeed, this putative NorF (with 61 a.a.) is 40 % shorter than its

297   homologues. However, the analysis of the entire intergenic region between *MARHY3057* and

298   *MARHY3058* identifies a longer ORF encoding a protein with 79 residues, that has 39 % primary

299   sequence identity with *P. stutzeri* NirP. Therefore, we propose that NorF is misannotated in *M.*

300   *hydrocarbonoclasticus* SP17 genome, being encoded in the 3141724-3141963 genomic region

301   rather than in the 3141778-3141963 region.

302   A second *norB* gene (*MARHY3014*) also encoding a NOR is annotated in *M.*

303   *hydrocarbonoclasticus* genome, downstream the *nos* cluster and transcribed in the opposite

304   direction (see Figure S3 in Supplementary Information). This NOR is composed of a single long-

305   chain subunit being a *q*-NOR homologue (primary sequence identity with *Geobacillus*

306   *stearothermophilus* *q*-NOR is 37 %, with a 95 % coverage, and 25 % with *P. aeruginosa* large

307   subunit NorB, but with only 60 % coverage) (Table S2 in Supplementary Information). While *c*-

308   NOR uses a *c*-type cytochrome as electron donor, *q*-NOR accepts electrons from the quinone

309 pool. The presence of two types of NOR in the same bacteria does not seem to be frequent

310 (Heylen et al. 2007; Jones et al. 2008) and its biological relevance is unknown.

311 After the *norBC* genes, a large cluster of 10 genes involved in the nitrite reduction step of the

312 denitrification pathway was found linked together, *nirFCSDLGHJEN*. Different genetic

313 arrangements of *nir* genes have been identified in bacteria. *P. aeruginosa* presents the most

314 similar genetic organization of the nitrite reductase gene cluster in comparison to the one of *M.*

315 *hydrocarbonoclasticus* (Bali et al. 2014; Philippot 2002). The only differences are in the *nirM*

316 gene, encoding cytochrome c_{551}, which is absent in *M. hydrocarbonoclasticus* and in *nirFC*,

317 which are located upstream *nirS* and are transcribed in the opposite direction. NirM is the

318 electron donor of NiR in *P. aeruginosa*, while the cytochrome c_{552}, encoded by *MARHY3556*,

319 was identified as the physiological electron donor of NiR in *M. hydrocarbonoclasticus* (Lopes et

320 al. 2001) and is distantly located in the genome.

321 The denitrification pathway has been proposed to be regulated mainly by transcription regulators

322 of the CRP/FNR family, FNR and DNR, that in *M. hydrocarbonoclasticus* are encoded by

323 *MARHY0862* (FNR homologue) and *MARHY3023* (DNR homologue), with this later ORF being

324 located upstream the *nos* gene cluster. FNR, that activates genes during anaerobiosis, is a

325 homodimer containing a [4Fe-4S] center per protomer, which is sensitive to oxygen and to

326 nitrosylation (Crack et al. 2014). On the other hand, DNR senses N-oxides, in particular NO

327 (Arai et al. 1999), through a heme (Castiglione et al. 2009). These two transcription regulators

328 bind specifically to consensus sequences of the type $TTGATN_4ATCAA$ (named FNR binding

329 box). Thus, the promoter regions of the four gene clusters were analyzed to identify the presence

330 of these binding boxes, up to 200 bp upstream their ATG site. Homologous consensus sequences

331 were identified based on its score and distance to the putative transcription site (Figure 2). For

332   most of the gene clusters, the putative binding regions are located around -60 to -90 bp, except

333   for *nirSDLGH* (-162.5 bp) and *dnr* (-121.5 bp). These distances are in agreement with the

334   average location of these sites identified in the whole genome of *P. aeruginosa* (Trunk et al.

335   2010) and also with the more common spacing locations observed for FNR in *E. coli*, which are

336   usually centered at approximately -41, -61, -71, -82 and -92 bp from the transcription initiation

337   point (Wing et al. 1995). Although these binding sites still need to be experimentally confirmed,

338   the involvement of MARHY0862 (FNR homologue) and MARHY3023 (DNR homologue) in

339   the regulation of the denitrification pathway will be discussed.

340   The other regulatory system of denitrification is NarXL that responds to nitrate and is proposed

341   to be involved in the regulation of the *nar* genes (Schreiber et al. 2007). NarL, the transcription

342   regulator recognizes specific heptameric motifs (TACYYMT) with a 7-2-7 arrangement located

343   in the promoter regions of *nar* gene cluster (Schreiber et al. 2007). The promoter region of *narK*

344   and *narGHJV* was analyzed to identify the -10 and -35 boxes, which were only found upstream

345   *narK*, which lead us to propose that *narKGHJV* is transcribed into a single polycistronic unit.

346   Moreover, upstream *narK* a potential NarL binding site (around -21 bp, TACCCCA, with a score

347   of 4.13 for NarL of *E. coli*) and a FNR/DNR binding site were identified but none on *narGHJV*

348   (Figure 2). Relative to *narXL*, no binding sites for FNR/DNR nor NarL were identified upstream

349   the -10/-35 boxes, which can indicate that these genes are constitutive. Moreover, NarL is not

350   involved in regulation of *dnr* as no consensus sequences were identified upstream of FNR box,

351   as opposite to what was described for *P. stutzeri* (Härtig et al. 1999) (*dnrE*) and *P. aeruginosa*

352   (*dnr*) (Schreiber et al. 2007) that carried the motifs and were shown to have a NarL-dependent

353   transcription.

354

Analysis of gene expression during *M. hydrocarbonoclasticus* 617 growth in the presence of

nitrate - microoxic batch growth

The expression of denitrification genes of *M. hydrocarbonoclasticus* 617 grown in the presence

of nitrate, in the 2 L-bioreactor, was analyzed by quantitative real-time PCR. The results

obtained for both *norB* genes (*MARHY3054* and *MARHY3014*) indicates that *norB_MARHY3054*

(*c-norB*) gene is the one transcribing an active nitric oxide reductase under the denitrifying

conditions used here, as no significant expression levels are observed for the *norB_MARHY3014*

(*q-norB*) gene in these conditions (Figure 3). Thus, *q*-type NOR (encoded by

norB_MARHY3014) does not contribute to the *M. hydrocarbonoclasticus* denitrification

pathway, under these conditions, and its role in the physiology of this microorganism remains

unknown.

Expression profiles show that the genes encoding the catalytic subunits of the denitrifying

enzymes (*narG*, *nirS*, *norB_MARHY3054* and *nosZ*) are expressed simultaneously after 1 h, and

the maximum level of transcription occurs at time-point 5 h (end of the first diauxic phase), for

these four genes (Figure 3).

At 5 h of growth, *narG* expression level is slightly lower than the other genes (Figure 3),

reflecting the existence of additional regulatory mechanisms in *nar* expression or a lower

strength of the *fnr* promoter in the *nar* gene cluster.

Transcriptional analysis of *nos* gene cluster

In *M. hydrocarbonoclasticus nos* cluster is composed of *nosRZDFYL* (see Figure S2 in

Supplementary Information). The *nosR* and *nosZ* genes are separated by 75 bp, while 68 bp

separate *nosZ* from *nosD*. The *nosD*, *nosF* and *nosY* genes overlap each other by 2 bp and

378   finally, *nosY* and *nosL* are separated by 22 bp. This organization suggests that these genes might

379   be transcribed into a single transcriptional unit. To investigate this hypothesis reverse

380   transcription of total RNA, from a sample of the bioreactor, was performed and the intergenic

381   regions of the corresponding cDNAs were amplified by PCR. Amplicons with the expected sizes

382   were obtained from *nosR* and *nosZ*, *nosZ* and *nosD*, and *nosDFYL* intergenic regions (Figure 4A

383   and 4B), showing that *nosRZDFYL* is transcribed into a polycistronic unit, similarly to *P.*

384   *aeruginosa nos* gene cluster (Arai 2003).

385

386   ***Marinobacter hydrocarbonoclasticus* growth under denitrifying conditions**

387   *M. hydrocarbonoclasticus* is a ubiquitous marine bacterium that populates the subtropical area

388   and the Mediterranean Sea. In the present work, this bacterium was grown under two different

389   conditions, microoxic and anoxic, as a model for the metabolism occurring at two different sea

390   depths. The growth in the bioreactor was performed under microoxic conditions as a model for

391   the layers close to the surface, while the growth in the sealed serum flasks are a model for deeper

392   sea layers.

393   *(i) Growth in a bioreactor under microoxic conditions*

394   *M. hydrocarbonoclasticus* cultures were performed in a 2-L bioreactor under microoxic

395   conditions (low aeration rate) and in the presence of nitrate (10 mM), to promote denitrification

396   (2017; Eady et al. 2016; Zumft 1997). The analysis of the growth curve shows the presence of a

397   diauxic growth. The first growth phase occurs without any lag phase during the first 5 h with a

398   growth rate of 0.173 ± 0.008 h^{-1}, slowing down (growth rate of 0.011 ± 0.001 h^{-1}) until

399   approximately 35 h, when it reaches the stationary phase (Figure 5A). The lag phase was not

400   observed in any of the replicated assays, indicating that adaptation-period was not required, or it

401   was very small; and the death phase was not reached even after 48 h of growth, suggesting that

402   the carbon source, lactate, had not been completely consumed.

403   The oxygen level was monitored during the growth, showing a rapid decrease in the first 2 h, and

404   remaining negligible until the end of the growth (see Figure S2 in Supplementary Information).

405   This apparent absence of oxygen does not mean that there is no oxygen, but that the amount

406   dissolved is being completely consumed: the low aeration rate combined with the low agitation

407   at 50 rpm after 5 h of growth will lower the amount of dissolved oxygen in the growth media.

408   This foresees that the microorganisms will grow in microenvironments experiencing anoxic or

409   near anoxic conditions.

410   A diauxic growth was reported for *P. denitrificans* during anoxic growth in the presence of

411   nitrate (60 mM) (Hahnke et al. 2014), with the first corresponding to the consumption of nitrate

412   and the second with the start of nitrite consumption. However, in the present study the two

413   exponential phases seem to correspond to the simultaneous use of oxygen and nitrate as terminal

414   electron acceptors by *M. hydrocarbonoclasticus*, in the first phase, and in the sole use of the low

415   amount of oxygen dissolved in the growth media in the second exponential phase, with the first

416   having an expected energetic advantage.

417   *(ii) Growth in sealed serum flasks*

418   *M. hydrocarbonoclasticus* was grown in sealed serum flasks in a medium with the same

419   composition and under similar condition of agitation (in this case orbital shaking). Inspection of

420   the growth curve indicates that the exponential phase starts one hour after inoculation and has a

421   duration of 5 h, with a growth rate of 0.22 ± 0.02 h^{-1} (Figure 5B), as the first growth phase of the

422   microoxic growth. The stationary phase occurs after this time-point and lasts until 50 h of

423   growth, without observation of a death phase.

424

425 **Activity profile of denitrifying enzymes**

426 Nitrate and nitrite were quantified during *M. hydrocarbonoclasticus* growth, to monitor the

427 action of NaR and cd_1NiR, respectively, which catalyze the first and second steps of the

428 denitrification pathway (Figure 1). In addition, the reduction rate of nitric oxide and nitrous

429 oxide by whole-cells was also determined at different time-points during growth, to identify

430 when *c*-NOR and N_2OR were active in the cells (Figure 5).

431 The data obtained indicate that nitrate was being consumed in the second hour of the growth and

432 was completely consumed after 3 h (first mid-exponential phase of the diauxic growth and the

433 time-point at which the oxygen level is negligible, see Figure S1 in Supplementary Information).

434 This is an indication that nitrate transport to the cytoplasm and NaR were active before time-

435 point 2 h in the bioreactor. Indeed, at time-point 1 h, *narG* gene expression was already

436 occurring at low levels (Figure 3), and thus it is likely that NaR was already active in the cells.

437 Moreover, the decrease in nitrate concentration was concomitant with the formation of nitrite,

438 which reaches a maximum after 3 h of growth with a value close to the initial nitrate

439 concentration (8.5 mM), and four hours later (during the initial stages of the second diauxic

440 growth phase) nitrite was completely consumed (Figure 5A). This decrease in nitrite

441 concentration is attributed to the activity of cd_1NiR. In fact, a correlation between *nirS*

442 expression and nitrite consumption is observed (Figure 3 and 5A). Moreover, similar nitrate and

443 nitrite profiles were observed for the growth in the sealed serum flasks, indicating that both

444 enzymes are also active under these conditions (Figure 5B).

445 The last two steps of the denitrification pathway are catalyzed by *c*-NOR and N_2OR, and to

446 determine if these enzymes are active in *M. hydrocarbonoclasticus* the reduction rate of NO and

447   N$_2$O by the whole-cells was monitored (Figure 5). The results obtained from the growth carried

448   in the bioreactor indicate that both enzymes started to be active in the cells after 5 h of growth.

449   Moreover, it was observed that these enzymes are active in the cells until the end of the growth

450   (Figure 5), even if NO and N$_2$O are expected to have been completely consumed earlier on

451   (Bergaust et al. 2010).

452   On the other hand, the profile of the reduction rate of NO and N$_2$O by the whole-cells grown in

453   the sealed serum flasks showed maximum NO reduction rate at 3 h, when high levels of nitrite

454   are still present in the medium, while the N$_2$O reduction was only observed after approximately 6

455   h of growth, indicating that both enzymes are active under these conditions at pH 7.5 (Figure

456   5B). Moreover, contrary to what was observed for the cells cultured in the bioreactor under

457   microoxic conditions, the ability to reduce these metabolites decreases towards the end of the

458   growth.

459

460   **Kinetic parameters for N$_2$O reduction by whole-cells**

461   The N$_2$O reduction by the whole-cells of *M. hydrocarbonoclasticus* as a function of substrate,

462   N$_2$O, has a hyperbolic behavior (Figure 4C). This data was fitted with a Michaelis-Menten

463   equation to estimate the kinetic parameters, V_{max} of 2.2 ± 0.1 μmol_{N2O} min^{-1} mg^{-1} and K_m of 18 ±

464   5 μM. This K_m is of the same order of magnitude as the K_m of Clade I *P. stutzeri* strain DCP-Os1

465   N$_2$OR (36 ± 9 μM) determined by N$_2$O consumption measurements, which are lower than those

466   reported for whole-cells containing Clade II N$_2$OR (1.0 ± 0.2 μM and 1.3 ± 0.4 μM, from

467   *Dechloromonas denitrificans* strain ED-1 and *Anaeromyxobacter dehalogenans* strain 2CP-C,

468   respectively) (Yoon et al. 2016).

469

470 **Discussion**

471 **Gene expression and regulation of denitrification in *M. hydrocarbonoclasticus***

472 In *M. hydrocarbonoclasticus* there is a 70 kb region that encodes all the genes involved in the

473 denitrification pathway (see Figure S3 in Supplementary Information), with the promoter regions

474 of these gene clusters presenting a FNR/DNR consensus sequences, while NarL binding

475 sequences were only identified upstream the *nar* operon (Figure 2).

476 The genome of this bacterium has genes that encode two different types of NORs, *q*-NOR and *c*-

477 NOR, but under the denitrifying conditions used here only the later catalytic gene subunit is

478 expressed at significant levels (Figure 3), and in fact this was the enzyme isolated from *M.*

479 *hydrocarbonoclasticus* membrane extracts (Timoteo et al. 2011).

480 In *M. hydrocarbonoclasticus*, the onset and maximum of *nosZ*, *nirS*, *narG* and *norB* transcription

481 occurs simultaneously, which suggests that a common signal(s) triggers and regulates the

482 expression of these genes. The triggering signal can be the oxygen, which levels are very low

483 during the growth in the bioreactor (Figure S1, Supplementary Information). This behavior is

484 different from the one in *P. denitrificans*, in which it was observed that *nosZ* is expressed earlier

485 than *nirS* and *norB* (Bergaust et al. 2010). Those authors interpreted this pattern of transcription

486 by *nosZ* transcription being triggered by oxygen, while the onset of *nirS* and *norB* transcription

487 was associated with the increase in nitric oxide concentration that occurs afterwards (Bergaust et

488 al. 2010) (*vide infra*).

489 Relative to the regulation of *M. hydrocarbonoclasticus* *nar* genes, similarly to what was

490 observed in *P. stutzeri* (Härtig et al. 1999) and *P. aeruginosa* (Schreiber et al. 2007), these might

491 be under the regulation of *narXL*, a nitrate-responsive two-component system. This was

492 supported by the identification of NarL DNA binding sites in the promoter region of *nar* gene

493   cluster (Figure 2), as mentioned.

494   The data obtained here does not univocally identified the signals involved in the regulation of *M.*

495   *hydrocarbonoclasticus* denitrification genes. However, it is expected that the common effectors

496   are oxygen and nitric oxide, as identified in other denitrifying bacteria (Spiro 2012), through the

497   action of FNR and DNR, respectively. In fact, given the pattern of transcription observed for the

498   genes encoding the catalytic denitrifying subunit, it can be postulated that oxygen and nitric

499   oxide are the main effectors in this organism. Upon decrease of oxygen tension in the cultures,

500   FNR monomers with its [4Fe-4S] centers dimerize, becoming activate, and bind specific DNA

501   regions, activating the transcription of several genes required for the anoxic metabolism, which

502   include activation of *dnr* and *narGHJ* (Crack et al. 2013; Trunk et al. 2010). In turn, upon the

503   initial activity of cd_1NiR, originated from the initial low levels of *nirS* transcription, NO

504   concentration will increase by the reduction of nitrite, and DNR will activate *nir*, *nor* and *nos*

505   genes (Figure 6). On the other hand, *nar* genes would be regulated by oxygen and nitrate that

506   activates their expression through *narXL*.

507   The existence of a cascade type regulation for these genes will prevent the accumulation of

508   intermediate toxic products. Although, FNR and DNR recognize the same promoter regions (as

509   mentioned before), it has been shown that DNR is the specific regulator of denitrification (Ebert

510   et al. 2017; Trunk et al. 2010). The mechanism for the discrimination of these binding sites is

511   still unknown, though nitrosylation of FNR could play a role, as upon nitrosylation (which might

512   occur when nitric oxide concentration increases), FNR reduces its binding affinity to the specific

513   DNA regions (Crack et al. 2013). This double regulatory mechanism might be important to avoid

514   increasing release of toxic nitric oxide by NiR, together with down-regulation of *nir*, *nor* and *nos*

515   gene clusters, as with a second regulator, as DNR, denitrification can proceed by activating those

516   gene clusters.

517

518   **Metabolites and NO/N$_2$O reduction rates by whole-cells**

519   Nitrate and nitrite concentration during the growth of *M. hydrocarbonoclasticus* was monitored,

520   being observed a rapid consumption of nitrate with concomitant formation of nitrite, which is

521   completely consumed after 2 h, in both types of growth conditions tested. Considering that the

522   decrease in nitrite concentration is due to cd_1NiR activity, as the denitrification pathway is

523   active, the concomitant formation of nitric oxide is expected, followed by formation of N$_2$O. The

524   activity of the two last enzymes of the denitrification pathway was proven by the observation of

525   the NO and N$_2$O reduction rate by the whole-cells, which occurs until the end of the growth

526   (Figure 5).

527   There was a delay between maximum gene expression (*nirS*, *norB* and *nosZ*) and enzymatic

528   activity or complete nitrite consumption: (i) *nirS* maximum expression occurs at 5 h and

529   complete consumption of nitrite occurs only after time-point 8 h; and (ii) *nosZ* and *norB*

530   maximum expression occurs at 5 h, while ability of the cells to reduce NO and N$_2$O is maximum

531   at 7 h. This displacement can be attributed to the maturation process of these three enzymes, as

532   *c*-NOR is a membrane-bound enzyme and, cd_1NiR and N$_2$OR catalytic center assembly involves

533   several accessory factors.

534   Comparison between the activity profiles obtained for the two types of growth showed that lower

535   reduction rates, especial of N$_2$O, are obtained in the sealed serum flasks. Two major explanations

536   can be hypothesized, either there is reduced transcription of *nosZ* genes under this condition or

537   the amount of N$_2$OR produced is lower. In fact, the yield of N$_2$OR isolated from a batch

538   bioreactor operated under microoxic conditions is 2.6 ± 0.4 mg/L medium, while from a similar

539   growth under anoxic conditions is 0.5 ± 0.3 mg/L medium.

540   Nevertheless, since cells isolated from both growth conditions were able to reduce nitrous oxide,

541   it is plausible to argue that *M. hydrocarbonoclasticus* can carry out the four steps of the

542   denitrification pathway under these two growth conditions, and this organism has a denitrifying

543   chain as the one schematically presented in Figure 1.

544

545   **N$_2$OR Clade and nitrous oxide affinity**

546   *M. hydrocarbonoclasticus* has an affinity for nitrous oxide consistent with the presence of a

547   Clade I N$_2$OR, which also agrees with the arrangement and gene constitution of *nos* operon in

548   this organism, *nosRZDFYL* (Figure 4B). Furthermore, the estimated K_m for N$_2$O reduction by the

549   whole-cells (18 ± 5 µM) (Figure 4C) is similar to the value reported for the N$_2$O reduction by the

550   *in vitro* activated fully-reduced N$_2$OR (K_m of 14 ± 3 µM) (Dell'acqua et al. 2008). Considering

551   that 40 µL of growth under microoxic conditions has a reduction rate of 3.4×10^{-2} µmol$_{N2O}$min^{-1}

552   (before being collected), and 1.49×10^{-4} mg of N$_2$OR (considering a 70 % recovery for the

553   isolation of N$_2$OR from this growth), this gives an estimate of 228 µmol$_{N2O}$ min^{-1} mg$_{N2OR}$$^{-1}$ for

554   the cells *in vivo*. This value is in fact similar to the specific activity of N$_2$OR in the activated

555   fully reduced form (200 µmol$_{N2O}$ min^{-1} mg$_{N2OR}$$^{-1}$) (Johnston et al. 2014). In the case of the anoxic

556   growth, an activity of the same order of magnitude as that one was estimated at the end of the

557   growth (340 µmol$_{N2O}$ min^{-1} mg$_{N2OR}$$^{-1}$).

558

559   **Conclusions**

560   *M. hydrocarbonoclasticus* presents in its genome all the genes encoding the catalytic subunits of

561   enzymes responsible for each step of the denitrification pathway. These genes, as well as those

562   encoding accessory factors, necessary for enzyme maturation, transcriptional regulators and

563   substrate transporters, were found to be organized in a common *locus*. Genetic clustering of

564   denitrification genes has been previously described for other bacteria, but clustering of genes

565   encoding the four denitrifying reductases, as observed in *M. hydrocarbonoclasticus*, seems to be

566   less frequent (Demanèche et al. 2009; Philippot 2002). Such genomic arrangement of

567   denitrification genes favors the hypothesis of the existence of "denitrification islands" that can be

568   transferred horizontally across species (Zumft 1997).

569   In the growth performed in the bioreactor under microoxic conditions in the presence of nitrate,

570   the genes encoding the catalytic subunits of denitrifying enzymes have a maximum expression

571   level at the end of the first diauxic phase (around 5 h, 2-3 h after oxygen levels reach its

572   minimum value), which rapidly decreases to very low levels. Thus, we propose that the initial

573   regulatory signal is oxygen, through a FNR-like transcriptional regulator (MARHY0862) that

574   activates the DNR-type transcription regulator (MARHY3023). This transcription regulator

575   responds to NO, a secondary signal, formed by NiR and that will regulate the expression of *nir*,

576   *nor* and *nos* clusters. The other secondary regulatory effector is nitrate, involved in the regulation

577   of *nar* genes expression, through the two-component system NarXL (Figure 6).

578   In both type of growths, nitrate consumption occurs in the early hours of the growth, while nitrite

579   consumption, and the ability of the whole-cells to reduce nitric and nitrous oxide occurs later (at

580   5 h of growth). This delay can be attributed to the requirement in accessory factors for the

581   maturation of these enzymes to produce an active enzyme.

582   Moreover, our data indicate that *c*-NOR and N_2OR are active until the end of the growth (48-50

583   h) in both type of growths. Thus, a functional denitrification pathway in *M.*

584   *hydrocarbonoclasticus* is observed from nitrate to dinitrogen gas under these growth conditions.

585 *M. hydrocarbonoclasticus* has a Clade I N_2OR, as the whole-cells have 18 ± 5 µM affinity for

586 N_2O, corroborating the gene composition and organization of *nos* operon, which is transcribed as

587 polycistronic unit, and it was estimated that the whole-cells present an activity per amount of

588 N_2OR that is consistent with the specific activity of the isolated enzyme upon activation.

589 *M. hydrocarbonoclasticus* is one of the major species that populates the subtropical oceans and

590 the Mediterranean Sea. The metabolism is modulated by the availability of oxygen in these

591 facultative anaerobes, with the oxygen tension decreasing with the sea depth. Therefore, to

592 mimic two natural growth conditions (lower sea depth and surface sea layers), this organism was

593 grown under microoxic (bioreactor) and anoxic (sealed serum flasks) conditions. Our data shows

594 that under both conditions the enzymes that catalyze the four steps of denitrification is active.

595 These data and methodology will be used in the future to monitor other effects on the

596 denitrification pathway of this organism, such as temperature and pH.

597

598

599

**Manuscript to be reviewed**

600 **References**

601

602 Moura I, Moura JJG, Pauleta SR, and Maia LB(Eds). 2017. *Metalloenzymes in Denitrification:*
603 *Applications and Environmental Impacts*. London: RSC.

604 Applied-Biosystems. 2004. Applied Biosystems Tutorial - Guide to Performing Relative
605 Quantitation of Gene Expression Using Real-Time Quantitative PCR. .

606 Arai H. 2003. Transcriptional regulation of the nos genes for nitrous oxide reductase in
607 Pseudomonas aeruginosa. *Microbiology* 149:29-36. 10.1099/mic.0.25936-0:
608 10.1099/mic.0.25936-0

609 Arai H, Kodama T, and Igarashi Y. 1999. Effect of nitrogen oxides on expression of the nir and
610 nor genes for denitrification in Pseudomonas aeruginosa. *FEMS Microbiol Lett* 170:19-24.

611 Bali S, Palmer DJ, Schroeder S, Ferguson SJ, and Warren MJ. 2014. Recent advances in the
612 biosynthesis of modified tetrapyrroles: the discovery of an alternative pathway for the formation
613 of heme and heme d 1. *Cell Mol Life Sci* 71:2837-2863. 10.1007/s00018-014-1563-x:
614 10.1007/s00018-014-1563-x

615 Bange HW. 2006. New Directions: The importance of oceanic nitrous oxide emissions.
616 *Atmospheric Environment* 40:198-199. 10.1016/j.atmosenv.2005.09.030:
617 10.1016/j.atmosenv.2005.09.030

618 1986. *The Prokaryotes. A Handbook on Habitats Isolation and Identification of Bacteria*: New
619 york: springer-verlag.

620 Bergaust L, Mao Y, Bakken LR, and Frostegård A. 2010. Denitrification response patterns
621 during the transition to anoxic respiration and posttranscriptional effects of suboptimal pH on

622   nitrous oxide reductase in Paracoccus denitrificans. *Appl Environ Microbiol* 76:6387-6396.

623   10.1128/aem.00608-10: 10.1128/aem.00608-10

624   Castiglione N, Rinaldo S, Giardina G, and Cutruzzolà F. 2009. The transcription factor DNR

625   from Pseudomonas aeruginosa specifically requires nitric oxide and haem for the activation of a

626   target promoter in Escherichia coli. *Microbiology* 155:2838-2844. 10.1099/mic.0.028027-0:

627   10.1099/mic.0.028027-0

628   Correia C, Besson S, Brondino CD, Gonzalez PJ, Fauque G, Lampreia J, Moura I, and Moura JJ.

629   2008. Biochemical and spectroscopic characterization of the membrane-bound nitrate reductase

630   from Marinobacter hydrocarbonoclasticus 617. *J Biol Inorg Chem* 13:1321-1333.

631   10.1007/s00775-008-0416-1: 10.1007/s00775-008-0416-1

632   Crack JC, Green J, Thomson AJ, and Le Brun NE. 2014. Iron-sulfur clusters as biological

633   sensors: the chemistry of reactions with molecular oxygen and nitric oxide. *Acc Chem Res*

634   47:3196-3205. 10.1021/ar5002507: 10.1021/ar5002507

635   Crack JC, Stapleton MR, Green J, Thomson AJ, and Le Brun NE. 2013. Mechanism of [4Fe-

636   4S](Cys)4 cluster nitrosylation is conserved among NO-responsive regulators. *J Biol Chem*

637   288:11492-11502. 10.1074/jbc.M112.439901: 10.1074/jbc.M112.439901

638   Dell'acqua S, Moura I, Moura JJ, and Pauleta SR. 2011. The electron transfer complex between

639   nitrous oxide reductase and its electron donors. *J Biol Inorg Chem* 16:1241-1254.

640   10.1007/s00775-011-0812-9: 10.1007/s00775-011-0812-9

641   Dell'acqua S, Pauleta SR, Monzani E, Pereira AS, Casella L, Moura JJ, and Moura I. 2008.

642   Electron transfer complex between nitrous oxide reductase and cytochrome c552 from

643   Pseudomonas nautica: kinetic, nuclear magnetic resonance, and docking studies. *Biochemistry*

644   47:10852-10862. 10.1021/bi801375q: 10.1021/bi801375q

645 Dell'Acqua S, Pauleta SR, Moura JJ, and Moura I. 2012. Biochemical characterization of the
646 purple form of Marinobacter hydrocarbonoclasticus nitrous oxide reductase. *Philos Trans R Soc*
647 *Lond B Biol Sci* 367:1204-1212. 10.1098/rstb.2011.0311: 10.1098/rstb.2011.0311

648 Demanèche S, Philippot L, David MM, Navarro E, Vogel TM, and Simonet P. 2009.
649 Characterization of denitrification gene clusters of soil bacteria via a metagenomic approach.
650 *Appl Environ Microbiol* 75:534-537. 10.1128/aem.01706-08: 10.1128/aem.01706-08

651 Eady RR, Antonyuk SV, and Hasnain SS. 2016. Fresh insight to functioning of selected enzymes
652 of the nitrogen cycle. *Curr Opin Chem Biol* 31:103-112. 10.1016/j.cbpa.2016.02.009:
653 10.1016/j.cbpa.2016.02.009

654 Ebert M, Laass S, Thurmer A, Roselius L, Eckweiler D, Daniel R, Hartig E, and Jahn D. 2017.
655 FnrL and Three Dnr Regulators Are Used for the Metabolic Adaptation to Low Oxygen Tension
656 in Dinoroseobacter shibae. *Front Microbiol* 8:642. 10.3389/fmicb.2017.00642:
657 10.3389/fmicb.2017.00642

658 Gomes JP, Hsia RC, Mead S, Borrego MJ, and Dean D. 2005. Immunoreactivity and differential
659 developmental expression of known and putative Chlamydia trachomatis membrane proteins for
660 biologically variant serovars representing distinct disease groups. *Microbes Infect* 7:410-420.
661 10.1016/j.micinf.2004.11.014: 10.1016/j.micinf.2004.11.014

662 Grimaud R, Ghiglione JF, Cagnon C, Lauga B, Vaysse PJ, Rodriguez-Blanco A, Mangenot S,
663 Cruveiller S, Barbe V, Duran R, Wu LF, Talla E, Bonin P, and Michotey V. 2012. Genome
664 sequence of the marine bacterium Marinobacter hydrocarbonoclasticus SP17, which forms
665 biofilms on hydrophobic organic compounds. *J Bacteriol* 194:3539-3540. 10.1128/JB.00500-12:
666 10.1128/JB.00500-12

667 Hahnke SM, Moosmann P, Erb TJ, and Strous M. 2014. An improved medium for the anaerobic
668 growth of Paracoccus denitrificans Pd1222. *Front Microbiol* 5:18. 10.3389/fmicb.2014.00018:
669 10.3389/fmicb.2014.00018

670 Härtig E, Schiek U, Vollack KU, and Zumft WG. 1999. Nitrate and nitrite control of respiratory

671 nitrate reduction in denitrifying Pseudomonas stutzeri by a two-component regulatory system

672 homologous to NarXL of Escherichia coli. *J Bacteriol* 181:3658-3665.

673 Heylen K, Vanparys B, Gevers D, Wittebolle L, Boon N, and De Vos P. 2007. Nitric oxide

674 reductase (norB) gene sequence analysis reveals discrepancies with nitrite reductase (nir) gene

675 phylogeny in cultivated denitrifiers. *Environ Microbiol* 9:1072-1077. 10.1111/j.1462-

676 2920.2006.01194.x: 10.1111/j.1462-2920.2006.01194.x

677 Jia W, Tovell N, Clegg S, Trimmer M, and Cole J. 2009. A single channel for nitrate uptake,

678 nitrite export and nitrite uptake by Escherichia coli NarU and a role for NirC in nitrite export and

679 uptake. *Biochem J* 417:297-304. 10.1042/bj20080746: 10.1042/bj20080746

680 Johnston EM, Dell'Acqua S, Ramos S, Pauleta SR, Moura I, and Solomon EI. 2014.

681 Determination of the active form of the tetranuclear copper sulfur cluster in nitrous oxide

682 reductase. *J Am Chem Soc* 136:614-617. 10.1021/ja411500p: 10.1021/ja411500p

683 Jones CM, Stres B, Rosenquist M, and Hallin S. 2008. Phylogenetic analysis of nitrite, nitric

684 oxide, and nitrous oxide respiratory enzymes reveal a complex evolutionary history for

685 denitrification. *Mol Biol Evol* 25:1955-1966. 10.1093/molbev/msn146: 10.1093/molbev/msn146

686 Kaye JZ, and Baross JA. 2000. High incidence of halotolerant bacteria in Pacific hydrothermal-

687 vent and pelagic environments. *FEMS Microbiol Ecol* 32:249-260.

688 Kristjansson JK, and Hollocher TC. 1980. First practical assay for soluble nitrous oxide

689 reductase of denitrifying bacteria and a partial kinetic characterization. *J Biol Chem* 255:704-

690 707.

691 Laass S, Kleist S, Bill N, Druppel K, Kossmehl S, Wohlbrand L, Rabus R, Klein J, Rohde M,

692 Bartsch A, Wittmann C, Schmidt-Hohagen K, Tielen P, Jahn D, and Schomburg D. 2014. Gene

693 regulatory and metabolic adaptation processes of Dinoroseobacter shibae DFL12T during

694 oxygen depletion. *J Biol Chem* 289:13219-13231. 10.1074/jbc.M113.545004:
695 10.1074/jbc.M113.545004

696 Li R, Zi X, Wang X, Zhang X, Gao H, and Hu N. 2013. Marinobacter hydrocarbonoclasticus
697 NY-4, a novel denitrifying, moderately halophilic marine bacterium. *Springerplus* 2:346.
698 10.1186/2193-1801-2-346: 10.1186/2193-1801-2-346

699 Ling J, Lin L, Zhang Y, Lin X, Ahamad M, Zhou W, and Dong J. 2017. Draft Genome Sequence
700 of Marinobacter hydrocarbonoclasticus Strain STW2, a Polycyclic Aromatic Hydrocarbon-
701 Degrading and Denitrifying Bacterium from the Rhizosphere of Seagrass Enhalus acodoides.
702 *Genome Announc* 5. 10.1128/genomeA.01412-16: 10.1128/genomeA.01412-16

703 Lopes H, Besson S, Moura I, and Moura JJ. 2001. Kinetics of inter- and intramolecular electron
704 transfer of Pseudomonas nautica cytochrome cd1 nitrite reductase: regulation of the NO-bound
705 end product. *J Biol Inorg Chem* 6:55-62.

706 Marquez MC, and Ventosa A. 2005. Marinobacter hydrocarbonoclasticus Gauthier et al. 1992
707 and Marinobacter aquaeolei Nguyen et al. 1999 are heterotypic synonyms. *Int J Syst Evol*
708 *Microbiol* 55:1349-1351. 10.1099/ijs.0.63591-0: 10.1099/ijs.0.63591-0

709 Mauffrey F, Cucaita A, Constant P, and Villemur R. 2017. Denitrifying metabolism of the
710 methylotrophic marine bacterium Methylophaga nitratireducenticrescens strain JAM1. *PeerJ*
711 5:e4098. 10.7717/peerj.4098: 10.7717/peerj.4098

712 Mauffrey F, Martineau C, and Villemur R. 2015. Importance of the Two Dissimilatory (Nar)
713 Nitrate Reductases in the Growth and Nitrate Reduction of the Methylotrophic Marine Bacterium
714 Methylophaga nitratireducenticrescens JAM1. *Front Microbiol* 6:1475.
715 10.3389/fmicb.2015.01475: 10.3389/fmicb.2015.01475

716 Moir JW, and Wood NJ. 2001. Nitrate and nitrite transport in bacteria. *Cell Mol Life Sci* 58:215-
717 224.

718 Pauleta SR, Dell'Acqua S, and Moura I. 2013. Nitrous oxide reductase. *Coord Chem Rev*
719 257:332-349. 10.1016/j.ccr.2012.05.026: 10.1016/j.ccr.2012.05.026

720 Philippot L. 2002. Denitrifying genes in bacterial and Archaeal genomes. *Biochim Biophys Acta*
721 1577:355-376.

722 Prudêncio M, Pereira AS, Tavares P, Besson S, Cabrito I, Brown K, Samyn B, Devreese B, Van
723 Beeumen J, Rusnak F, Fauque G, Moura JJ, Tegoni M, Cambillau C, and Moura I. 2000.
724 Purification, characterization, and preliminary crystallographic study of copper-containing
725 nitrous oxide reductase from Pseudomonas nautica 617. *Biochemistry* 39:3899-3907.

726 Ramos S, Almeida RM, Cordas CM, Moura JJG, Pauleta SR, and Moura I. 2017. Insights into
727 the recognition and electron transfer steps in nitric oxide reductase from Marinobacter
728 hydrocarbonoclasticus. *J Inorg Biochem* 177:402-411. 10.1016/j.jinorgbio.2017.09.001:
729 10.1016/j.jinorgbio.2017.09.001

730 Schreiber K, Krieger R, Benkert B, Eschbach M, Arai H, Schobert M, and Jahn D. 2007. The
731 anaerobic regulatory network required for Pseudomonas aeruginosa nitrate respiration. *J
732 Bacteriol* 189:4310-4314. 10.1128/jb.00240-07: 10.1128/jb.00240-07

733 Singer E, Webb EA, Nelson WC, Heidelberg JF, Ivanova N, Pati A, and Edwards KJ. 2011.
734 Genomic potential of Marinobacter aquaeolei, a biogeochemical "opportunitroph". *Appl Environ
735 Microbiol* 77:2763-2771. 10.1128/AEM.01866-10: 10.1128/AEM.01866-10

736 Spiro S. 2012. Nitrous oxide production and consumption: regulation of gene expression by gas-
737 sensitive transcription factors. *Philos Trans R Soc Lond B Biol Sci* 367:1213-1225.
738 10.1098/rstb.2011.0309: 10.1098/rstb.2011.0309

739 Starkey RL. 1938. A study of spore formation and other morphological characteristics of vibrio
740 desulfuricans. *Archiv für Mikrobiologie* 9:268-304. 10.1007/bf00407364: 10.1007/bf00407364

741   Stein LY, and Klotz MG. 2011. Nitrifying and denitrifying pathways of methanotrophic bacteria.

742   *Biochem Soc Trans* 39:1826-1831. 10.1042/BST20110712: 10.1042/BST20110712

743   Timoteo CG, Pereira AS, Martins CE, Naik SG, Duarte AG, Moura JJ, Tavares P, Huynh BH,

744   and Moura I. 2011. Low-spin heme b(3) in the catalytic center of nitric oxide reductase from

745   Pseudomonas nautica. *Biochemistry* 50:4251-4262. 10.1021/bi101605p: 10.1021/bi101605p

746   Trunk K, Benkert B, Quack N, Munch R, Scheer M, Garbe J, Jansch L, Trost M, Wehland J,

747   Buer J, Jahn M, Schobert M, and Jahn D. 2010. Anaerobic adaptation in Pseudomonas

748   aeruginosa: definition of the Anr and Dnr regulons. *Environ Microbiol* 12:1719-1733.

749   10.1111/j.1462-2920.2010.02252.x: 10.1111/j.1462-2920.2010.02252.x

750   Untergasser A, Cutcutache I, Koressaar T, Ye J, Faircloth BC, Remm M, and Rozen SG. 2012.

751   Primer3—new capabilities and interfaces. *Nucleic Acids Res* 40:e115-e115. 10.1093/nar/gks596:

752   10.1093/nar/gks596

753   Wing HJ, Williams SM, and Busby SJ. 1995. Spacing requirements for transcription activation

754   by Escherichia coli FNR protein. *J Bacteriol* 177:6704-6710.

755   Yoon JH, Shin DY, Kim IG, Kang KH, and Park YH. 2003. Marinobacter litoralis sp. nov., a

756   moderately halophilic bacterium isolated from sea water from the East Sea in Korea. *Int J Syst*

757   *Evol Microbiol* 53:563-568. 10.1099/ijs.0.02363-0: 10.1099/ijs.0.02363-0

758   Yoon S, Nissen S, Park D, Sanford RA, and Loffler FE. 2016. Nitrous Oxide Reduction Kinetics

759   Distinguish Bacteria Harboring Clade I NosZ from Those Harboring Clade II NosZ. *Appl*

760   *Environ Microbiol* 82:3793-3800. 10.1128/AEM.00409-16: 10.1128/AEM.00409-16

761   Zumft WG. 1997. Cell biology and molecular basis of denitrification. *Microbiol Molec Biol Rev*

762   61:533-616.

763

764

Primers used in qPCR of genes encoding the denitrification enzymes andco-transcriptional analysis of the nitrous oxide reductase gene cluster.

1 **Table 1** – Primers used in qPCR of genes encoding the denitrification enzymes and co-

2 transcriptional analysis of the nitrous oxide reductase gene cluster.

Gene	Primer	Sequence (5'-3')	Amplified fragament (bp)
narG	narG_F	CCACCTCCTTCTTCTATGCTC	59
	narG_R	ATCCACGCCCAGTTTCTC	
nirS	nirS_F	GCGATGAAGTGTGGTTCTCT	56
	nirS_R	AACGATGGCGGATTTCTTGT	
q-norB (*MARHY3014*)	norB_F	GCTGAATACGACACCCACTC	59
	norB_R	CCAGGAAGCCATAAACACCA TGGTGTTTATGGCTTCCTGG	
c-norB (*MARHY3054*)	norB2_F	AGAAGCCCAGACCGAACT	60
	norB2_R	GCGAACACCCAGAACAGAAT ATTCTGTTCTGGGTGTTCGC	
nosZ	nosZ_R	CTGATGGCAAATGGCTGGT	56
	nosZ_F	CGGCAGGAAACGGTCTTT	
nosR	nosR_F	ACAGAAGCCGAAGATGATGC	50
	nosR_R	TGTAAACCAGGAAGCCGTG	
nosD	nosD_F*	GACTACCTGGGCTGGGAT	58
	nosD_R	TCGGTTCATAAGGCACATCG	
nosL	nosL_F	CTTTACCGAGCGAGAACAGA TGTCTTTGGTGGAGCAGAAT	50
	nosL_R*	ATTCTGCTCCACCAAAGACA	
16S rRNA	16S_F	TAACCTGGGAACGGCATTT	55
	16S_R	CCACTACCCTCTACCACACT	

3 **Note:** *PrimerS used to amplify the intergenic region between *nosD* and *nosL*.

Schematic representation of denitrification pathway in *M. hydrocarbonoclasticus*

Reactions catalyzed by those enzymes create a proton gradient across the membrane, generating a positive potential outside of the inner membrane. The electrons for each reaction come from the quinone pool. NDH and SDH are the NADH dehydrogenase and succinate dehydrogenase, respectively. Cyt is the abbreviation used for cytochrome and Moco for the molybdenum cofactor. IM and OM are the inner and outer membranes, respectively. Nitrate and nitrite type of transportation across the membrane is envisaged to be occur through NarK homologues.
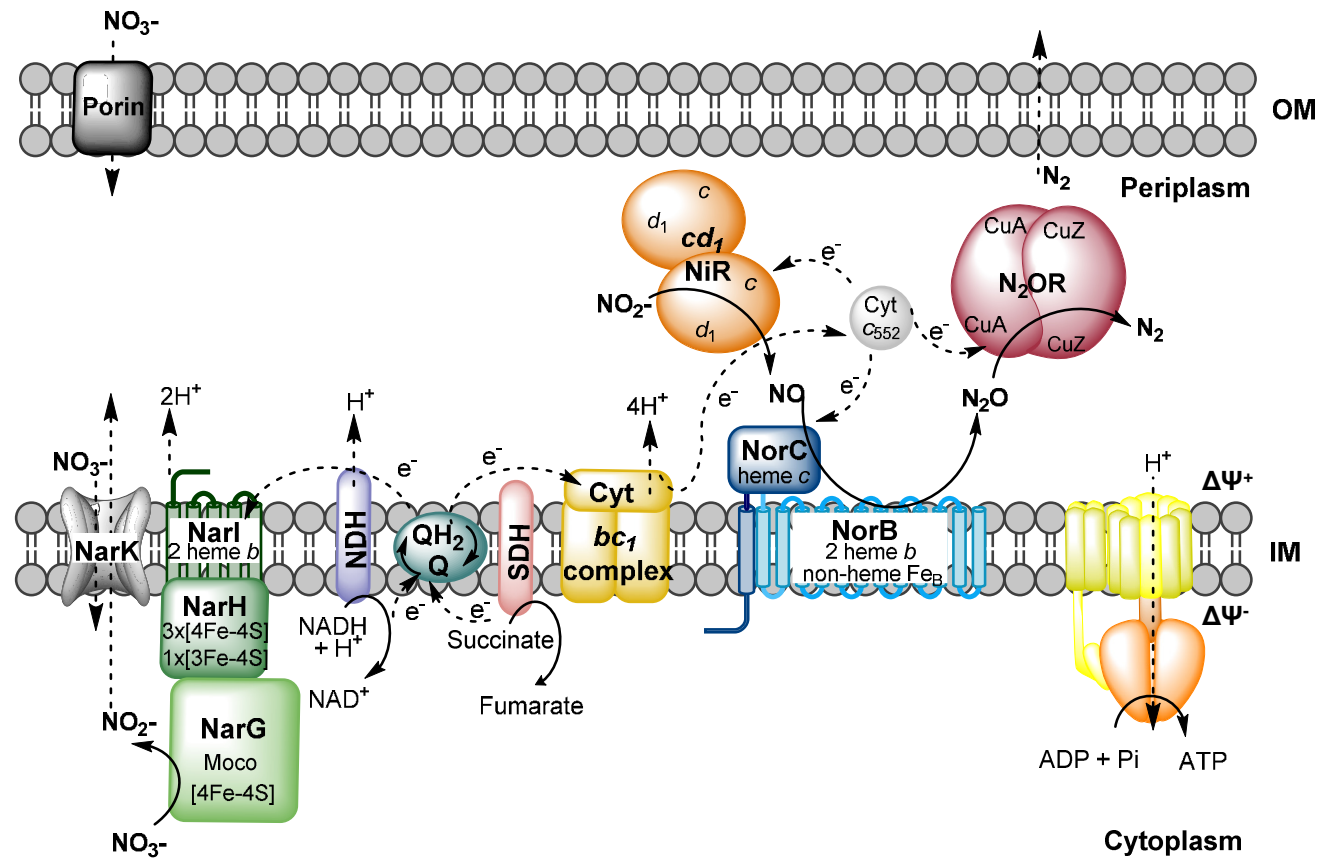
Figure 2

Analysis of the promoter regions of nitrate reductase (*nar*), nitrite reductase (*nir*), nitric oxide reductase (*nor*) and nitrous oxide reductase (*nos*) gene clusters.

Analysis of the promoter region of (A) *nar* , (B) nir, (C) *nor* and (D) *nos* genes. Sequence alignments between the identified putative FNR/DNR-binding sequences and the consensus sequence are shown, as well as its position from the putative transcription initiation site. The putative NarL binding site is evidenced in the *nar* cluster. A putative FNR/DNR box was identified in the promoter region of the *dnr* gene upstream *nos* gene cluster. For more details regarding genes belonging to each cluster please refer to Figure S3. Genes are not drawn to scale.
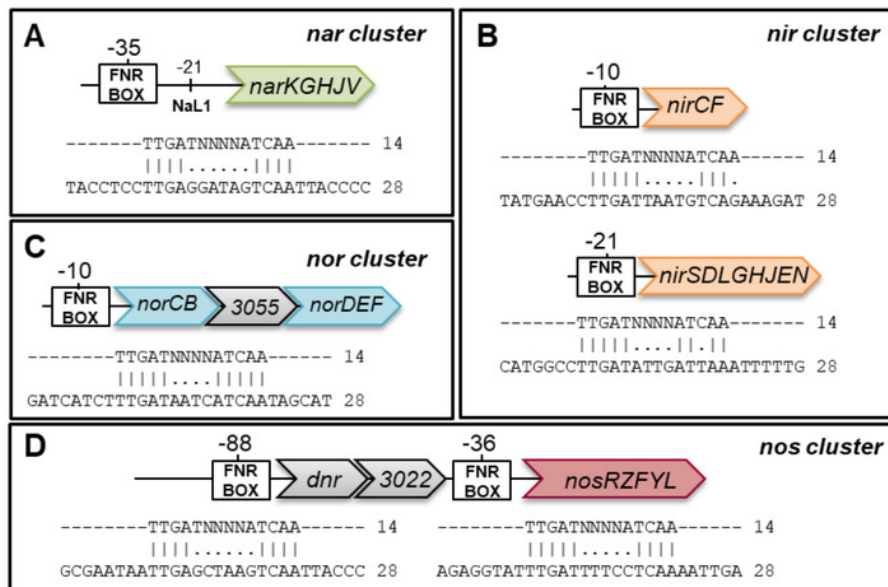
Figure 3

Profile of the expression levels of the genes encoding the catalytic domains of the denitrification enzymes.

Expression of *narG* (green squares), *nirS* (orange triangles), *c-norB* (blue filled circles), *q-norB* (blue open circles) and *nosZ* (red diamonds) encoding the catalytic domains of *M. hydrocarbonoclasticus* denitrification enzymes along the 50 h of growth under microaerobic conditions in the bioreactor. Relative expression values were obtained by normalizing expression of each target gene to the control housekeeping gene 16S rRNA, as described in Materials and Methods. Growth curve is represented as grey circles in the secondary axis.
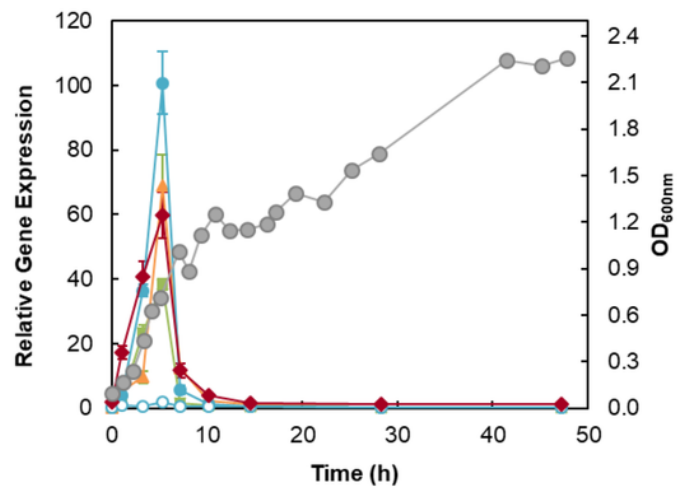
Figure 4

M. hydrocarbonoclasticus genome encodes a Clade I N$_2$OR

(A) Analysis of the transcriptional organization of *M. hydrocarbonoclasticus* nitrou s oxide reductase (*nos*) gene cluster. PCR products of intergenic regions between (a) *nosR-nosZ*, (b) *nosZ-nosD* and (c) *nosD-nosL* using cDNA (first lane), RT (minus) control reaction (second lane), genomic DNA (third lane) and water (fourth lane). No amplifications were obtained in the "RT-minus" control reaction, indicating that the amplification from cDNA samples was not due to the presence of contaminating genomic DNA. (B) Genomic organization of the *nos* gene cluster in the genome of *M. hydrocarbonoclasticus*. The gene encoding for N$_2$OR is colored in black. (C) Kinetic activity for the reduction of N$_2$O by the whole-cells of *M. hydrocarbonoclasticus* grown under microaerobic conditions in the presence of nitrate at pH 7.5. Data were fitted to Michaelis-Menten equation, using a K_m of 18 ± 5 µM and V_{max} 2.2 ± 0.1 µmol$_{N2O}$ min^{-1} mg^{-1} of total protein.
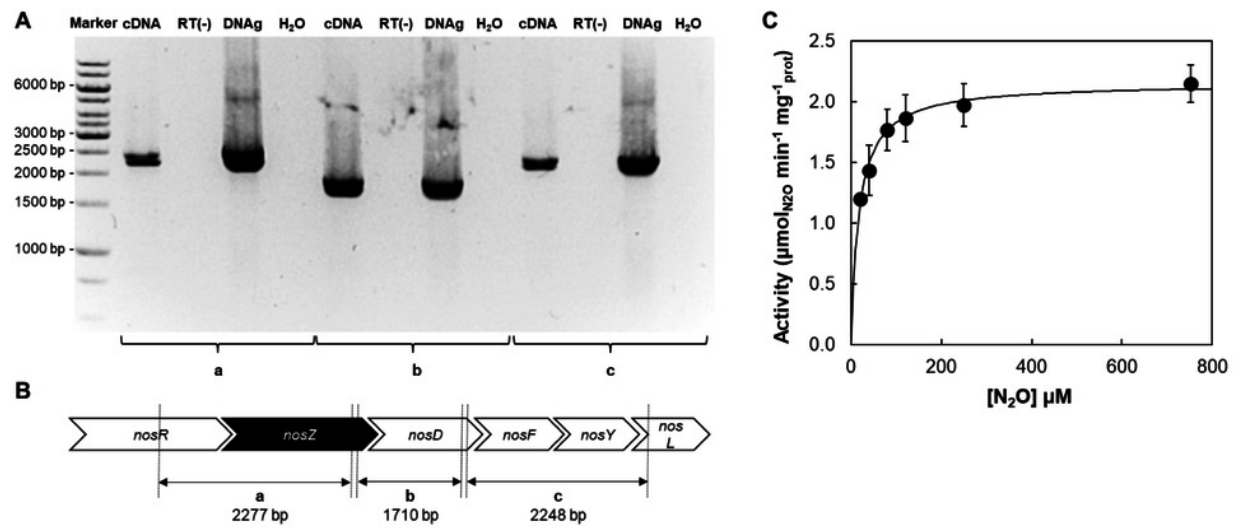
Figure 5

M. hydrocarbonoclasticus profile of denitrification pathway metabolites and enzyme activity.

Nitrate (green squares) and nitrite (orange triangles) concentrations (primary axis) and nitric oxide (blue circles) and nitrous oxide (red diamonds) reduction rates by the whole-cells determined at different time-points are shown in the secondary axis for the growth under microaerobic conditions in the bioreactor **(A)** or performed in sealed serum-flasks **(B)**. The activity is given as micromoles of NO or N_2O reduced per minute per optical density. The assays were performed as described in Materials and Methods, in triplicates. Three biological replicates were analyzed (for the data presented in this Figure) but not at the exact same time points, thus a representative experiment is shown (similar results were obtained for the other replicas). The growth curve of *M. hydrocarbonoclasticus* in the bioreactor (grey circles) and in the serum flasks (black open circles) is included in the additional axis in A and B, respectively.
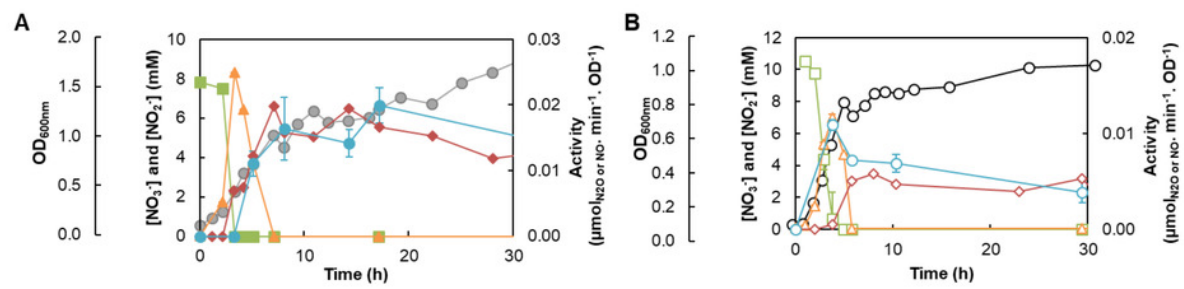
Figure 6

Putative regulatory network controlling denitrification gene expression in *M. hydrocarbonoclasticus*.

The main effector involved in regulation of nitrate reductase (*nar*), nitrite reductase (*nir*), nitric oxide reductase (*nor*) and nitrous oxide reductase (*nos*) gene clusters is the low oxygen tension through a FNR-type regulator. Secondary effectors are nitric oxide (NO) (first produced by the initial low levels of nitrite reductase) involved in expression regulation of *nir*, *nor* and *nos* genes clusters, through a DNR-type regulator, and nitrate (NO_3^-) involved in regulation of *nar* genes through the two-component system NarXL. Our own bioinformatic analyses suggest that MARHY0862 and MARHY3023 are, respectively, the FNR and DNR homologues involved in regulation of denitrification gene expression in *M. hydrocarbonoclasticus*. Dash lines indicate the putative but lower level of *nir*, *nor* and *nir* gene regulation by FNR.